Science of the Total Environment 796 (2021) 148818

Contents lists available at ScienceDirect

Science of the Total Environment

journal homepage: www.elsevier.com/locate/scitotenv

3D GIS for surface modelling of magnetic fields generated by overhead power lines and their validation in a complex urban area

Laia Miravet-Garret [a,*], Óscar David de Cózar-Macías [a], Elidia Beatriz Blázquez-Parra [a], Manuel Damián Marín-Granados [a], Juan Bernabé García-González [b]

[a] Department of Graphic Expression, Design and Projects, School of Industrial Engineering, University of Malaga, c / Doctor Ortiz Ramos s / n, 29071 Malaga, Spain
[b] Department of Electrical Engineering, School of Industrial Engineering, University of Malaga, c / Doctor Ortiz Ramos s / n, 29071 Malaga, Spain

HIGHLIGHTS

- An ELF-EMF surface has been provided on the actual terrain relief using 3D GIS.
- The use of a 5-m resolution DTM was essential.
- MAPE was 10% in a free urban area to 20% in a consolidated urban area.
- 86% of the control points were correctly classified according to usual percentiles of exposure.

GRAPHICAL ABSTRACT

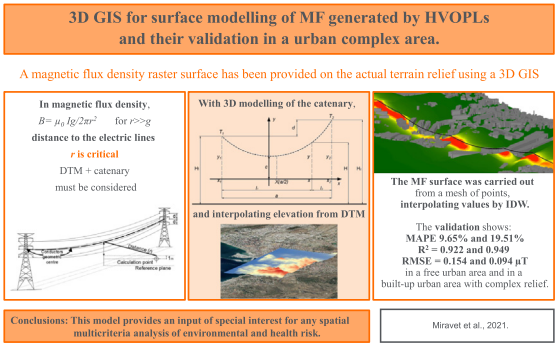

ARTICLE INFO

Article history:
Received 30 April 2021
Received in revised form 23 June 2021
Accepted 29 June 2021
Available online 10 July 2021

Editor: Philip K. Hopke

Keywords:
EMF
Overhead power lines
Exposure modelling
Geographical information system
Digital terrain model

ABSTRACT

Residential exposure to magnetic fields generated by overhead high-voltage power lines, continues to be a matter of social concern and, for the scientific community, a challenge to model this exposure accurately enough to reliably detect even small effects in large populations complexes. In any expression of the magnetic field intensity, the source-receiver distance is a determining variable, especially in an environment closer to the electrical installation and critical with the existence of significant unevenness in the terrain. However, MF exposure studies adopt, due to their complexity, simplifications of reality where even sometimes the terrain relief and the buckling of the line are not considered. The application of 3D techniques with Geographic Information Systems (GIS) allows us to address this problem. This article presents a model for generating magnetic field intensity surfaces from high-precision terrain elevation data. The series expansion of the Biot-Savart law to an infinite rectilinear conductor with variable height according to the catenary described by the cables using ArcGIS software is applied to calculate the magnetic field. For the validation, 69 control points (1035 field measurements) were used in a free urban area and another 28 points (420 field measurements) in a built-up urban area with complex relief. Good estimates were obtained, although with differences in both areas. With MAPE 9.65% and 19.51%, R2 = 0.922 and 0.949, RMSE = 0.154 and 0.094 μT, respectively. Furthermore, 86% of the points were correctly classified according to usual exposure percentiles. However, the use of a 5 m resolution digital terrain model to obtain high-precision elevation data was an indispensable condition for the good performance of our model. The result as a continuous surface of magnetic field values at the real elevation of the ground can contribute significantly to the development of new environmental and public health studies.
© 2021 The Authors. Published by Elsevier B.V. This is an open access article under the CC BY-NC-ND license (http://creativecommons.org/licenses/by-nc-nd/4.0/).

* Corresponding author.
E-mail addresses: laiamiravet@uma.es (L. Miravet-Garret), odecozar@uma.es (Ó.D. de Cózar-Macías), ebeatriz@uma.es (E.B. Blázquez-Parra), mdmarin@uma.es (M.D. Marín-Granados), jbgarcia@uma.es (J.B. García-González).

https://doi.org/10.1016/j.scitotenv.2021.148818
0048-9697/© 2021 The Authors. Published by Elsevier B.V. This is an open access article under the CC BY-NC-ND license (http://creativecommons.org/licenses/by-nc-nd/4.0/).

1. Introduction

The possible association of various serious diseases with prolonged exposure to extremely low frequency magnetic fields (ELF-MF) such as those produced by high-voltage overhead power lines (HVOPLs) has been a matter of social concern for several decades (European Commission, 2010; Furby et al., 1988; Lienert et al., 2017; Porsius et al., 2014; Repacholi, 2012). Since the late 1970s, a significant number of epidemiological studies have been carried out (Ahlbom et al., 2001; Kokate et al., 2016). Various pooled analyses (Ahlbom et al., 2000; Greenland et al., 2000) showed an increased risk of childhood leukaemia associated with relatively high-level values of residential exposure to these fields. Based on these facts, in 2001 the International Agency for Research on Cancer (IARC) classified low frequency magnetic fields as "possibly carcinogenic to humans" or Group 2B (IARC, 2002, 2013). This determination is applied when epidemiological evidence is "limited" and there is no biophysical mechanism capable of explaining the biological effects of magnetic fields (MF) at environmental exposure levels (WHO, 2007). A recent review of the scientific evidence available up to March 2015 (Schüz et al., 2016), has maintained this risk assessment. Therefore, due to this lack of specificity in the scientific community about the possible adverse effects of residential exposure to ELF-MF, it is necessary to continue research in order to confirm or rule out whether the association observed in epidemiological studies is due or not to a possible causal relationship (SCENHIR, 2015).

Spatial modelling of environmental pollutants is an important tool for epidemiologists to analyse the effects of exposures at the population level (Graham et al., 2004; Jerrett et al., 2010). In addition, in case and control studies of exposure to ELF-MF, the use of models based on calculated fields can reduce selection bias by not requiring the direct participation of the subjects to take personal MF measurements (Feychting, 2014; Teepen and van Dijck, 2012).

One of the main obstacles that epidemiological studies must face is the high difficulty of modelling the exposure to these fields. The intensity of the magnetic field at any point in the space generated by an overhead power line is a function of the intensity of the current in its circuits, the geometrical configuration and arrangement of the phases and the distance from that point to the conductors. The influence of this last parameter translates into a rapid drop in the field as one moves away from the power line at the rate of the inverse of the square or the cube of its value, depending on the wiring configuration.

Therefore, a geographical model for the estimation of magnetic field values must aspire to have a completely three-dimensional consideration, where the geometry of the line and its buckling, the terrain morphology and in particular, the relative distance between the calculation points and the electric line, are accurately reproduced and especially, in its proximity.

The studies that are carried out on large populations adopt, due to their complexity, certain simplifications of reality. The first studies were based on a design known as the cable code or Wertheimer-Leeper (WL) (Wertheimer and Leeper, 1979, 1982) that categorizes exposure based on proximity to the closer overhead power line and according to a series of related parameters such as voltage and wiring configuration. Later, other studies based solely on proximity emerged (Feychting and Alhbom, 1993). The one carried out in the United Kingdom (Draper et al., 2005) became a referent by indicating an association between dwellings close to overhead power lines with cases of childhood leukaemia and has been replicated in other large populations (Crespi et al., 2016; Pedersen et al., 2014b; Sermage-Faure et al., 2013) and in combination with other possible environmental risk factors, such as radon, air pollution caused by traffic or pesticide exposure (Hoffmann et al., 2008; Pedersen et al., 2014a; Reynolds et al., 2001). A recent study carried out in California and the United Kingdom (Amoon et al., 2020) showed that, in this region, horizontal distance alone represented a proxy for magnetic field exposure within 100 m of the line. However, there are also several studies that have reported that proximity and WL indicators are not adequate predictors of exposure and that, therefore, the results of research carried out with these methodologies are not interpretable (Kheifets et al., 1997; Maslanyj et al., 2009; Rankin et al., 2002).

On the other hand, the studies that have applied 3D calculation methods generalize the catenary using common values for the clearance, and the terrain is considered completely flat and horizontal. The geographical relief is only considered at less than 50 m from the line through estimates obtained in visits to the site (Swanson, 2008; Tynes and Haldorsen, 1997) or they incorporate the topography by applying a correction factor to the magnetic field values previously obtained also from a model without any elevation (Bessou et al., 2013). Other authors make 3D models by collecting data from the power line and the locations of the dwellings of interest using rangefinders and Global Positioning System (GPS) (Vergara et al., 2015). Collecting field data requires an investment of considerable resources and time.

In all these types of epidemiological studies, the calculation of magnetic fields is carried out using very specific software or provided by the company that owns the power lines not always accessible to the scientific community in general.

Geographic Information Systems (GIS) are a common tool with great potential in environmental health studies. In magnetic contamination studies, the most common GIS applications include geocoding procedures for case study addresses and control (Kheifets et al., 2015) horizontal distance estimation of these cases to the power lines (Pedersen et al., 2014b; Vergara et al., 2015) and the integration of results obtained with other specific software (Najjar et al., 2009) for their subsequent territorial analysis. Some studies have developed interactive applications integrated in GIS environments that allow calculating field values using three-dimensional equations (Turgeon et al., 1998) and modelling magnetic field surfaces using 3D finite element mesh generators from the power line input data (Joseph et al., 2018) although the terrain elevation data is not incorporated.

In this work, a map of magnetic flux density values generated by HVOPLs is developed from a 3D geographic model entirely by means of a GIS, where an accurate representation of the catenary described by the cables, as well as high precision topographic data for the entire study area are included. In this way, the real distances between the ground points and the power line, and consequently the magnetic field for any terrain altitude, are reproduced with significant accuracy even in areas with complex geographical reliefs.

The expression of the results as a continuous field of values not only allows estimations of the magnetic flux density in the dwellings of case studies and control, but also is a fundamental tool to follow government recommendations for making electromagnetic exposure maps lines available to the public (European Parliament, 2009) and for urban planning of safe distances from dwellings to power lines (PACE, 2011). Likewise, it provides input for any spatial multicriteria analysis of environmental and health risk assessment where other pollutants of a continuous geographical nature intervene, allowing to obtain more complete maps of environmental quality.

Finally, the model has been validated by measurements in an urban area with a wide variety of buildings and a complex geographical relief, based on data provided by the company in charge of managing the line.

This document is structured as follows: Section 2 presents the methods and materials used to model the magnetic field surface and its validation. In Section 3, the results of the magnetic field values measured in the field and the reciprocals modelled are collected, as well as the results corresponding to the validation of the model. Section 4 includes the discussion of the study; and Section 5 presents the general conclusions.

2. Materials and methods

2.1. Model

2.1.1. Magnetic field calculation method

To calculate the magnetic field, a useful method is used to estimate exposure levels (Cruz-Romero, 2000) consisting of the series expansion

of the Biot-Savart law applied to indefinite rectilinear conductors (Kaune and Zaffanella, 1992). To reduce the error caused by substituting the catenary for a line, the height of this line is made to coincide with that of the catenary for each point where it is measured (Mamishev et al., 1996). The relative height between the calculation point and the catenary is given by the difference in altitude between the point according to the terrain and a section of the catenary produced by a transverse plane that passes through the point (Fig. 1). The calculation points have been set at 1 m above the ground, this being a recommended standard (IEEE Std 644-1994, 1994; UNE 215001:2004, 2004). The expressions of magnetic flux density *B (μT)* for various relative positions of the phase conductors in a vertical double circuit are given by (1):

$$B = \frac{\mu_0 \sqrt{3}\, d}{2\pi r^2} I_g \text{ for } r >> d \quad (1)$$

where μ_0 is the magnetic permeability of vacuum $(4\pi 10^{-4}\, T A / m)$, *d* is the separation between phases *(m)*, *Ig* represents a term that operates the current of the circuits depending on the *g* configuration of the phases *(A)*, and *r* is the distance between the calculation point and the geometric centre of the spatial arrangement of the phase conductors *(m)*, since in this way the magnetic field error is minimal (Cruz-Romero, 2000).

This applied magnetic field calculation method assumes that both circuits carry positive sequence currents, such as those in this study (Fig. 2). This model considers phase transposition, although induced currents in the ground and unbalanced currents induced in the circuits have not been taken into account.

2.1.2. 3D modelling of the study area

An urban area of the city of Malaga (Spain) with a residential character was chosen, which includes several schools and social services centres. The ground relief in the area is highly variable with orthometric altitudes between 9.5 m and 240.16 m. The urban typology according to the cadastral parcel includes buildings with multiple dwellings and single-family dwellings.

This zone is crossed by a 2.5 km section of the "Montes-Centro" HVOPL that connects the "Montes" electrical substation with the "Centro" underground power line, by means of two 66 kV circuits through eight spans. The delimitation of the study area was set at 1000 m from each side of the line.

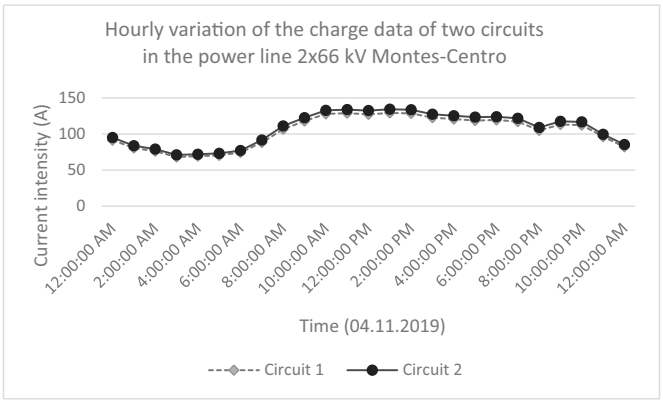

Fig. 2. Hourly variation of power line charge data.

This distance ensures the reduction of the magnetic field raised values generated by the reference overhead power line to negligible environmental values.

Some supports for the power line are located on hills that are difficult to access, sometimes surrounded by dense vegetation, while others are located at street level. The line is a three-phase double circuit with LA-280 conductors. The line charge data, as well as the supports coordinates, towers height, spacing and phases arrangement, cross-arms width and values of the cables mechanical tension were provided by the company e-Distribución Redes Digitales S.L.U. responsible for the installation.

In order to analyse in depth, the possible impact on this model of the precision of the digital terrain model used to represent the ground relief, two digital terrain models (DTM) were used: the "DTM05-LIDAR" with a 5 m wide mesh, with altimetric accuracy defined by values between 0.25 m and 0.5 m of root mean square error of the elevation (RMSEz) and with an estimated planimetric precision ≤0.5 m. The other one is a digital terrain model "DTM25" with a 25-m-wide mesh, thus following the same procedure as another similar study (Bürgi et al., 2017). Both DTMs, with edition date 2015, were obtained from the National Air Orography Plan of Spain. In this way, a catenary model was obtained for each case.

The digitalization of the catenary projection was carried out by joining the projections of the geometric centre of the phase's configuration in each support.

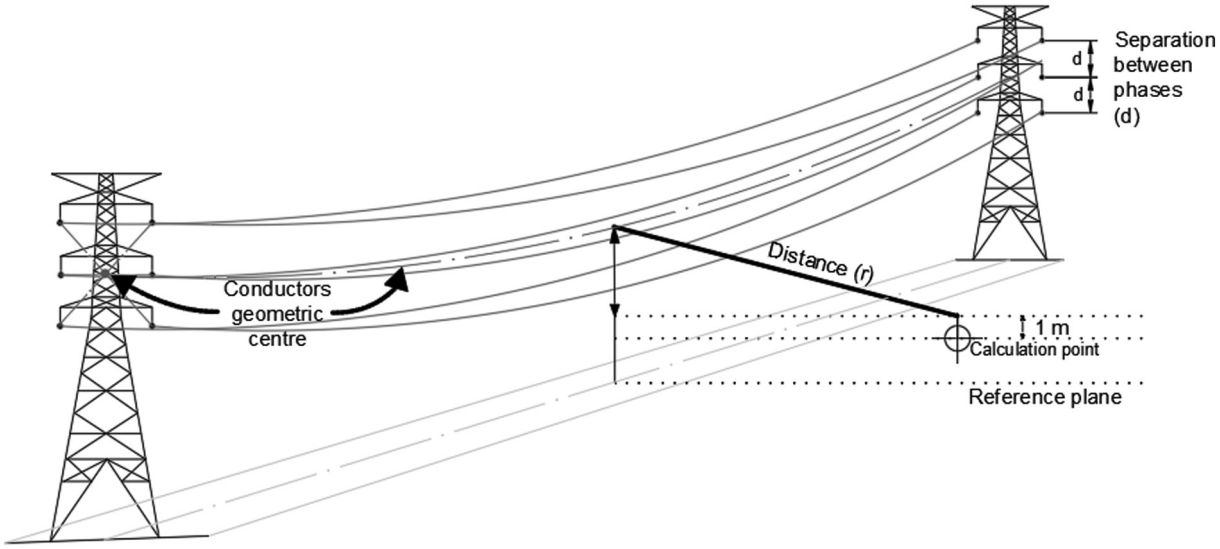

Fig. 1. Representation of the relative height between the geometric centre of the conductors and the measurement point according to the catenary.

To obtain the three-dimensional modelling of the catenary that describes the power lines, the line of each span was discretized as points with a separation of 0.5 m. The orthometric altitude H (m) of each of them in the curve they describe was calculated from their ordinate y (m) in the local axes of the catenary, given by expression (2):

$$y = c\cosh\frac{x}{c} = c\frac{e^{\frac{x}{c}} + e^{\frac{-x}{c}}}{2} \text{ where } c = \frac{T}{p} \quad (2)$$

c (m) is the constant of the curve given by the relationship between the mechanical horizontal component of the tension T (kg) and the weight per unit of cable length p (kg / m); x (m) the abscissa according to the coordinate axes of the catenary that pass through the vertex of the curve at a distance c from it (Fig. 3).

The determination of the abscissa x (3) of any point is possible if the abscissa X (m) of the midpoint of the span (4) and that of the supports x_1, x_2 is previously known (5):

$$x = x_1 + l_1 \text{ or } x = x_2 - l_2 \quad (3)$$

Being l_1 and l_2 (m) the horizontal distance from the point to supports 1 and 2 of its span, obtained for all the points of each span using a proximity tool,

$$X = c\,Asinhz = c\ln\left(z + \sqrt{z^2+1}\right) \quad \text{where } sinh\frac{X}{c} = \frac{d}{2csinh\frac{a}{2c}} = z \quad (4)$$

$$x_1 = X - \frac{a}{2}; x_2 = X + \frac{a}{2} \quad (5)$$

where a is the span length (m), obtained during the digitization process and d (m) represents the height difference of each span, given by the difference in orthometric altitudes of the geometric centres of the cable anchors. This altitude was estimated considering the one corresponding to the support base according to the digital model of the reference terrain, the free height of the support and the distance between phases. The transformation of the ordinate values of all the points of the catenary to values of orthometric altitudes H (6) could be obtained once both were known for a reference support of each span. The ordinate of the supports was obtained with (7):

$$H = y + (H_1 - y_1) \text{ or } H = y + (H_2 - y_2) \quad (6)$$

$$y_1 = c\,cosh\frac{x_1}{c}\ ; y_2 = c\,cosh\frac{x_2}{c} \quad (7)$$

With these equations, the ArcGIS software was able to obtain the three-dimensional modelling of the catenary calculating the orthometric altitude H of any of its points, where H1 and H2 have been obtained by adding to the orthometric height of the base of support 1 or 2, extracted of the DTM, the free height of that support and the distance between phases, provided by the electricity company.

The sag is dependent on several factors such as the cable temperature, which is influenced by the ohmic heating itself or by meteorological conditions, and by additional wind and snow loads, the latter being exceptional in the chosen study area. The temperature variation (±25 °C) throughout the year can produce changes of ±1 m of maximum deflection. However, the most extreme periods are short and although at maximum current charges the sinking of the line is also the highest, usually the circulating intensities are lower so that the geometric model of the line can be considered time independent.

2.1.3. Magnetic field surface modelling

The modelling of the magnetic field surface was carried out from a mesh of points. Three mesh densities were considered in order to compare results: 5 × 5 m and 10 × 10 m where the orthometric altitudes were derived from the DTM05, and one of 25 × 25 m where the altitudes were interpolated with the DTM25. The interpolation method applied was bilinear, since the elevation values are more adequately sampled using this method (ESRI, 2016). The values of minimum geometric distance between the mesh points and the overhead power line were obtained by means of proximity functions and the charge values of the line were averaged over the measurement time period. The magnetic field calculation for each point was carried out at one meter above the altitudes derived from the DTM, a value commonly used both for magnetic field measurements and for its calculation in epidemiological studies of residential exposure.

For each mesh, a magnetic field surface was generated by applying an inverse distance weighted (IDW) interpolation.

This interpolation method provides good results when the data set is abundant, they are homogeneously distributed, and their locations are close as in this case study. Also, as it is an exact interpolator, it guarantees that the input values are respected, and the result is always included within the variation range of the data. In a comparison of spatial interpolation methods for estimating electric field magnitudes, the IDW obtained the best results (Azpurua and dos Ramos, 2010). It was also used for the orographic evaluation of the magnetic field in other magnetic induction field estimation software (Comelli et al., 2007).

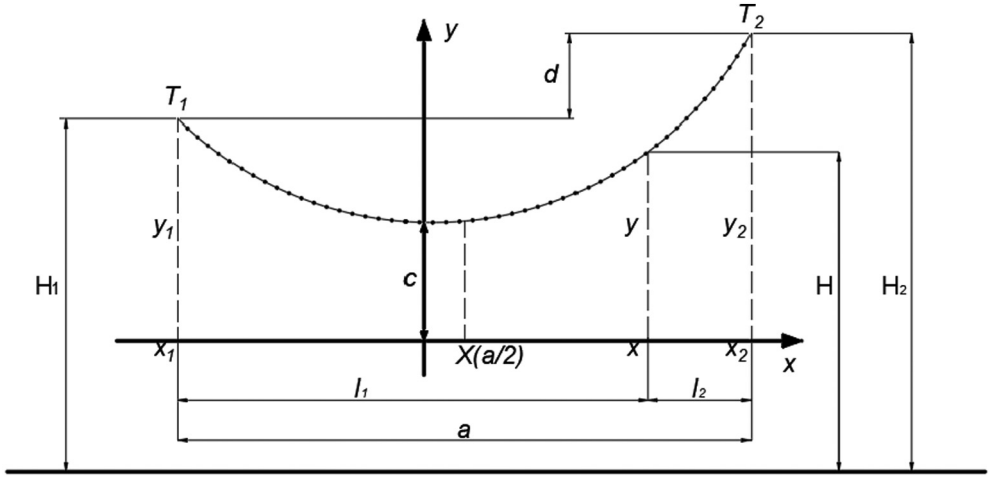

Fig. 3. Representation of the catenary in its local coordinate system and referencing the ordinates at orthometric altitudes.

2.2. Validation of the magnetic field surface

2.2.1. Magnetic field values measurement procedures

The objective of the validation procedure was to obtain a representative number of magnetic field reference values. The first site chosen for taking measurements within the study area was an urban free space on the border with an urban residential area. The height of the lowest conductors above the ground was approximately 11 m. The trajectory of the catenary in this validation area presents a very gentle slope despite the significant difference in level within the 100 m span.

69 points were reassessed in the field in 8 cross-sectional profiles 5 m apart from each other (Fig. 4).

Measurements were made in each lateral transect from the centre of the line at ±2.5 m, ±5 m, ±7.5 m, ±12.5 m and ±17.5 m. This maximum distance was imposed by the conditions of the terrain and the nearby constructions. The measurement of magnetic flux density values was carried out on Thursday, April 11, 2019 between 8:00 and 15:00 h. The procedure followed met the standards in force for this purpose (IEEE Std 644-1994, 1994; UNE 215001:2004, 2004).

Five measurements for each axis were taken in each location 1 m above the ground and the exact time of the measurement was recorded for each of them. Other values such as ambient temperature and humidity were also noted. The device used was a PCE-G28 triaxial magnetic field meter operating in a frequency range of 30 Hz to 300 Hz, with a resolution of 0.01 μT and a precision of "±4% + 0.03 μT" in a measurement range from 0.01 μT to 20 μT (PCE Instruments, 2014).

Given that one of the main objectives of this work is to develop a methodology to obtain magnetic field surfaces applicable to epidemiological studies, it seemed reasonable to also carry out a validation in a consolidated urban residential area. To this end, 28 street level control points were defined near to dwellings accesses. Given that in urban areas the measured values of the magnetic field can be influenced by other sources of magnetic induction that are not directly observable, efforts were made to select their locations as far as possible from manholes, control cabinets and other facilities. Likewise, the points were conveniently distributed on the map in order to preserve the spatial independence of errors. This measurement period was carried out on the same day between 16:00 and 20:00 h, also recording 5 values of magnetic flux density for each location and the exact time of the data measurement. The map of these control points is shown in Fig. 4.

The resultant magnetic field at any location was given by the expression:

$$B = \sqrt{B_x^2 + B_y^2 + B_z^2} \tag{8}$$

where Bx, By and Bz are the root-mean-square (rms) values of the three orthogonal field components.

2.2.2. Statistical evaluation of the model uncertainty

To evaluate the model reliability, a linear regression analysis and an analysis of differences were performed between the observed and the estimated values from each surface generated. The regression coefficient S, the determination coefficient R^2 and the root mean square error (RMSE) were obtained, as well as the mean relative error (MRE) (9) with its standard deviation (SD) and the mean absolute percentage error (MAPE) (10):

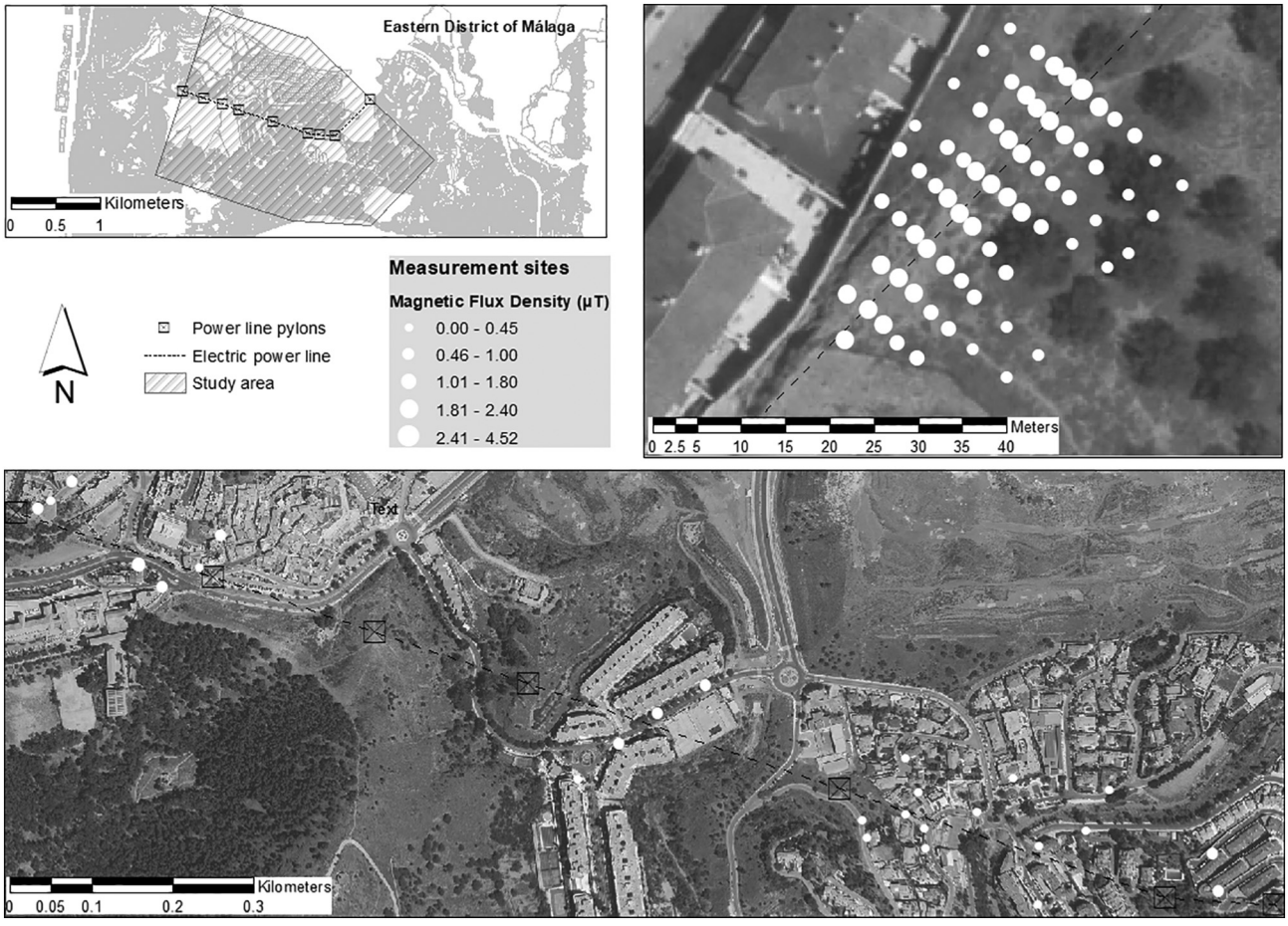

Fig. 4. Measurement sites distributed in lateral transects to the power line in the urban free zone (top right figure) and measurement sites distributed in the consolidated urban residential zone (bottom figure).

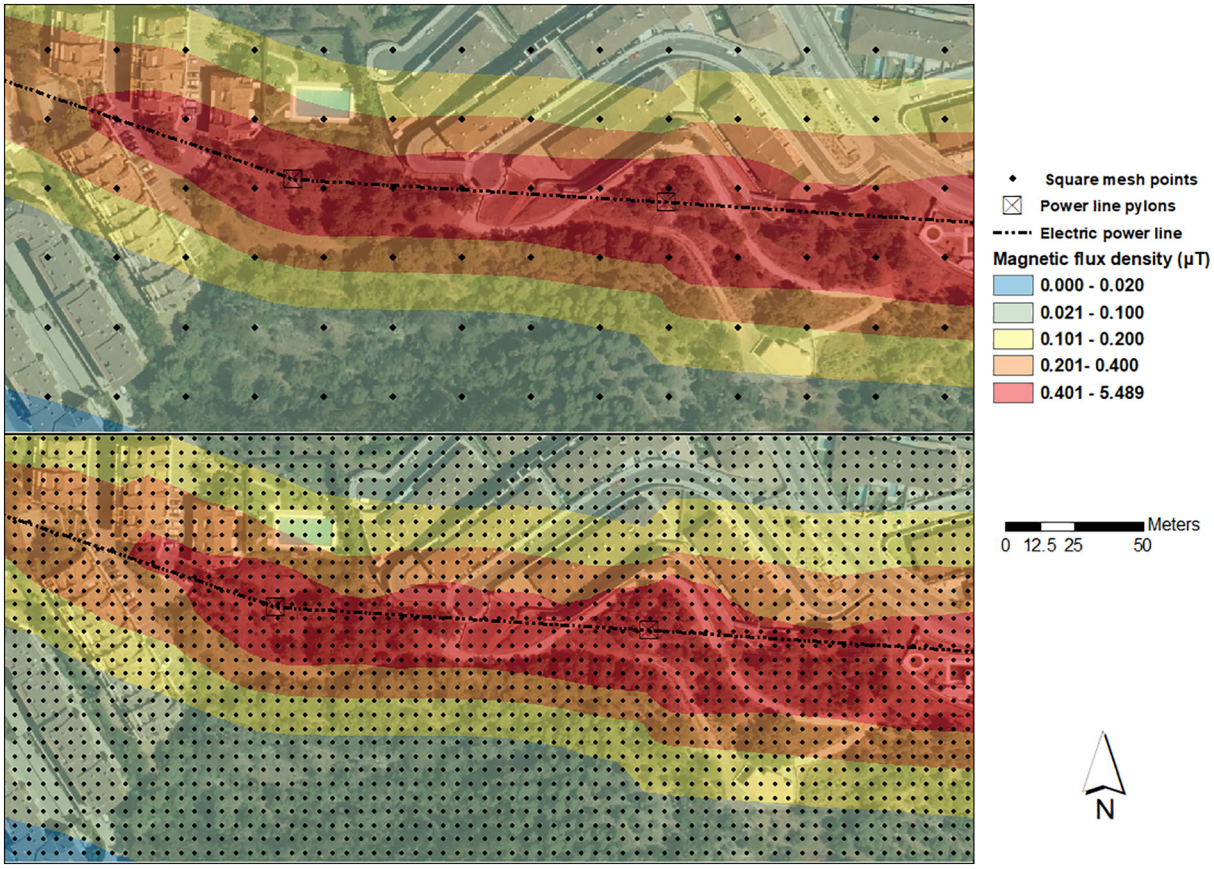

Fig. 5. Magnetic field surfaces generated by an overhead power line for a 25 m mesh (top) and a 10 m mesh (bottom).

$$\mathrm{MRE} = \frac{1}{n} \times \frac{B\,(model) - B\,(measured)}{B\,(measured)} \times 100 \tag{9}$$

$$\mathrm{MAPE} = \frac{1}{n} \times \frac{|B\,(model) - B\,(measured)|}{B\,(measured)} \times 100 \tag{10}$$

where the value of $B\,(measured)$ at a given point is the arithmetic average of its five values registered during the observation, and the $B\,(model)$ value is the one obtained through a bilinear interpolation for that same point from the calculated magnetic field surface.

The use of these two non-scale dependent error indexes is logical since the order of magnitude of the measured magnetic field values B (μT) varies depending on the distance from the point of measurement to the power line. In addition, they not only allow comparisons between the different model results both within and outside each urban context examined, but they allow also a more rigorous interpretation of their particular

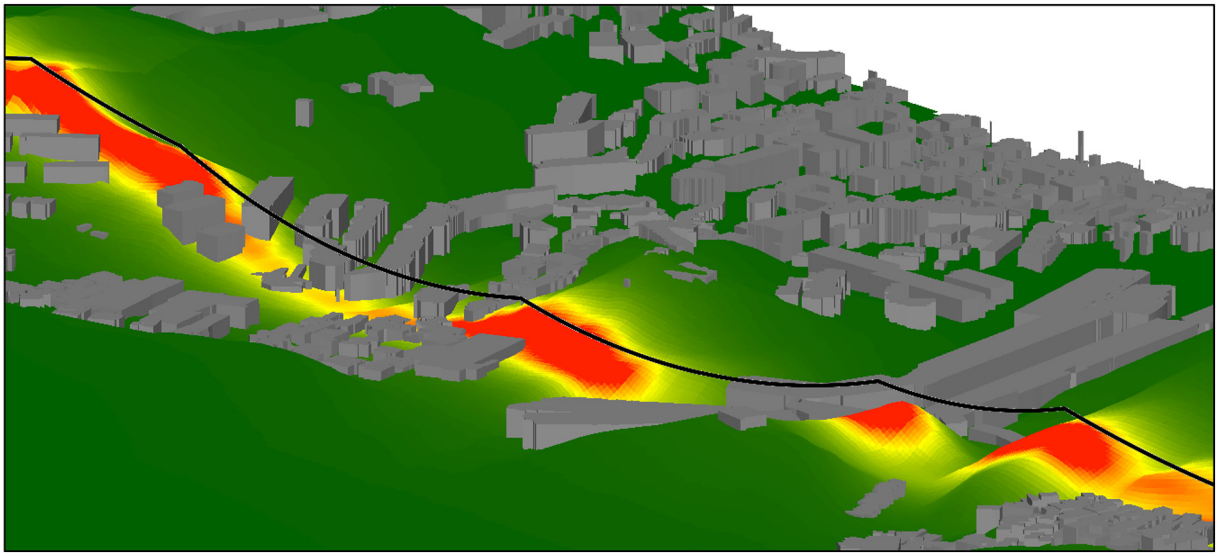

Fig. 6. 3D visualisation of the 5 × 5 m surface of magnetic field estimated at 1 m above the orthometric heights of the DTM05.

Table 1
Summary of results observed in the free zone and in the residential area.

Zone	N	B Minimum (μT)	B Maximum (μT)	B Average (μT)
Urban Free	69	0.453	2.432	1.056
Urban Residential	28	0.048	1.297	0.449

performance, since the results of the correlation alone are not consistently related to the precision of the simulation model (Willmott, 1982).

3. Results

3.1. Modelled surfaces

Given that the current values in the conductors were averaged according to the recorded values during the measurement period in each validation zone, the modelled surfaces represent the average exposure to ELF-MF during that time frame.

Fig. 5 shows an extract of the mesh obtained with 10 m resolution (upper image) and with 25 m resolution (lower image) superimposed on the magnetic field surfaces generated from of each one. Both surfaces share categorization ranges of magnetic field values. This allows to observe both the effect of the terrain, that can be appreciated by the lack of symmetry of the magnetic field surface along the axis corresponding to the layout of the power line, as well as the precision of the starting elevation data, evidenced through a greater contour irregularity of the area that represents higher values (red colour) when higher precision data are used.

The effect of the terrain becomes even more evident when making a representation of the magnetic field surface adjusted to its digital elevation model represented three-dimensionally (Fig. 6), where the influence of the ground relief combined with the line sag is clearly observed.

3.2. Measured values

8 lateral transects of the power line were obtained but only for 4 of them (profiles number 5, 6, 7 and 8) the terrain and urban conditions of the area allowed an analysis with the same number of measurement points. A summary of the results of the recorded measurements is shown in Table 1, where the maximum value of 2.432 μT measured directly under the line tracing drops to a minimum value of 0.453 μT at approximately 17 m from it.

The observations in the urban residential area showed lower values because the measurement points were located in wider ranges away from the line, and the separation of the cables from the ground was greater. The maximum value in this case was 1.297 μT measured next to a support of the electrical line located on the pavement and the minimum value was 0.048 μT at a horizontal distance of approximately 100 m from the electrical line.

3.3. Comparison of measured values with modelled values

The graphs of the registered magnetic field values at control points arranged in profiles transverse to the line showed the irregularity of the terrain. The smoothing of the real slopes that takes place in the digital terrain models provided more parabolic curves for the modelled B values. Although the recording of values for each control point was performed asynchronously, the variations of the line charge data during each measurement period were insignificant.

The comparison of the measured magnetic B values with those derived from each surface can be seen in Fig. 7. It is observed that the values derived from the surface generated with the DTM25 present a more significant overestimation. The models made from the DTM05 showed a notable fit to the measured values, the results being very similar for the mesh of 5 × 5 m and 10 × 10 m.

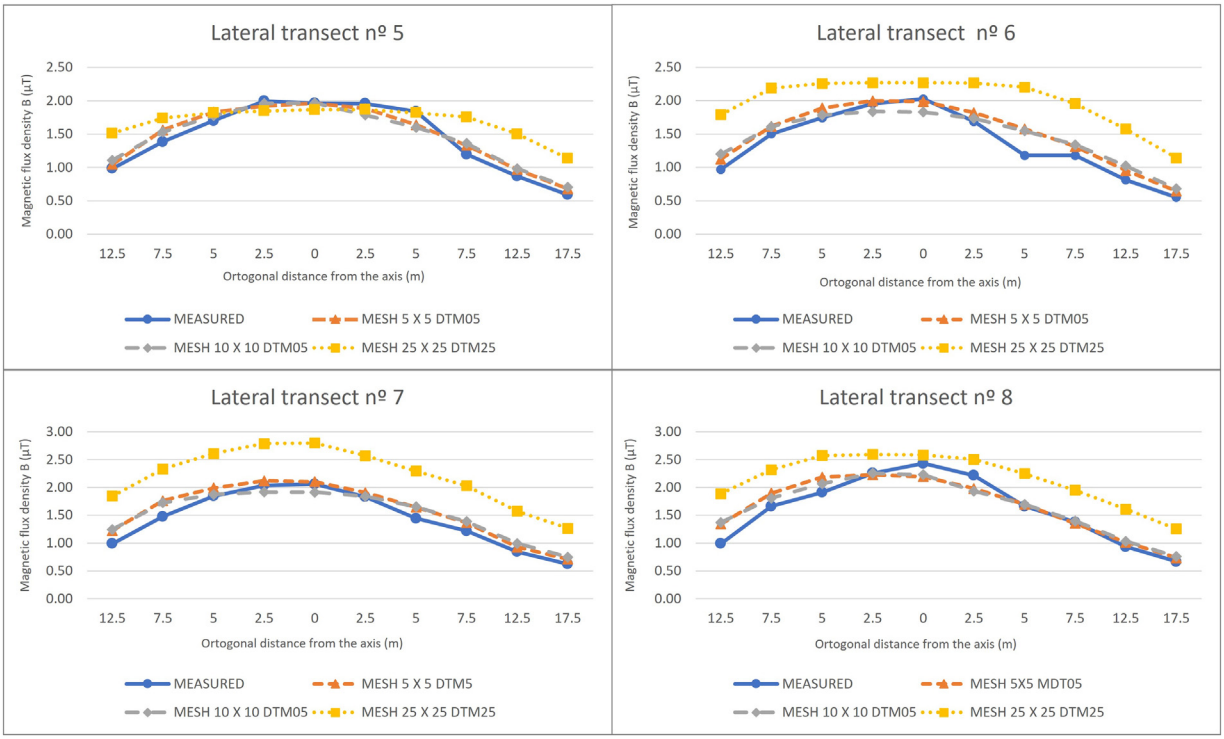

Fig. 7. Comparative graphs of the measured and modelled magnetic field values in profiles transverse to the line.

Table 2
Results of the statistical analyses for the model validation.

Zone	Model	MRE (%)	SD (%)	MAPE (%)	RMSE (μT)	R^2	S
Urban Free	Mesh space 5 × 5 DTM05	6.26	11.77	9.65	0.154	0.922	1.097
(Transverse Profiles)	Mesh space 10 × 10 DTM05	3.71	14.22	10.71	0.181	0.889	1.233
$N = 69$	Mesh space 25 × 25 DTM25	24.88	40.46	36.61	0.531	0.275	0.534
Urban Residential	Mesh space 5 × 5 DTM05	14.01	21.4	19.51	0.094	0.949	0.968
(Random locations)	Mesh space 10 × 10 DTM05	14.02	21.9	20.24	0.103	0.931	0.995
$N = 28$	Mesh space 25 × 25 DTM25	35.42	36.6	41.45	0.185	0.842	0.898

It was also observed when comparing the data that, for the finest models, from 17.5 m to the axis of the line, the differences with the observed values became minimal and their curves tend to coincide very closely from 12.5 m, especially on the far side of buildings.

From the results of the statistical analyses (Table 2) carried out for the validation of the modelled surfaces, it was again deduced that the behaviour of the model was significantly more precise when using the digital terrain model with 5-m resolution (DTM05) as input. A significant influence was not evident when generating the output with a mesh space of 5 m or 10 m. The differences analysis in these cases showed a very good response of the model in the urban free zone, although a decrease in the simulation quality was revealed in the more built-up area. The mean percentage error (MAPE) was doubled, its values 19.51% and 9.65% (5 × 5 mesh) and 20.24% and 10.71% (10 × 10 mesh). The difference between validation zones was less pronounced for the 25 × 25 mesh, with 41.45% and 36.61% in the residential area and in the free zone respectively. The positive MREs in all cases, for both validation zones, indicated the tendency of the three surfaces generated to overestimate the B values, again with greater differences and data dispersions in the residential area.

When the validation of the surfaces was carried out through cross-sectional profiles, the surface with the highest resolution obtained an MRE higher than that carried out with 10 m, with 6.26% (SD = 11.77%) and 3.71% (SD = 15.22%) respectively. This is because, although these results consider the global sense of the prediction, the errors in each reference point can be both positive and negative, and it may be the case that, even when these errors have significant magnitudes, the value of the relative mean error can be close to zero because they cancel each other.

In both cases, the results of the linear regression analysis showed an excellent fit of the modelled data to those observed with $R^2 = 0.949$ (5 × 5 mesh) and $R^2 = 0.931$ (10 × 10 mesh). The latter surface presents a mean change in the estimated values. Slightly more increased, according to S = 1.097 (5 × 5 mesh) and S = 1.233 (10 × 10 mesh). However, the fit of the model when working with ground data with 25 m resolution was poor, with $R^2 = 0.275$ and S = 0.53, as well as the result of its RMSE = 0.532 μT.

The behaviour of the model according to the data recorded in the residential area showed good adjustment, in this case with values of R^2 between 0.943 for the 5 × 5 mesh and 0.842 for the 25 × 25 mesh, as well as more homogeneous results between the different models also for the RMSE. This homogeneity, which does not appear when applying the other urban simulation condition, may be because the differences in the B values are higher in this area, but the increase in these differences between modelled surfaces when going down to the minimum resolution tested is less marked, and also extreme values dissolve faster in thicker resolutions (Pontius et al., 2008).

A better understanding of the model behaviour in connection with the distance to the centre of the power line was obtained from the scatter diagrams (Fig. 8) of the modelled values with respect to the measured values. For the three proposed surfaces, it can be observed that the adjustment tends to improve as the magnetic field values decrease, both in the urban free zone and in the residential urban zone. It is also observed that this gain is less pronounced within this last zone when the models originated with different terrain elevation accuracies are compared.

3.4. Adequacy of exposure levels

Given the possible applications of this work to future epidemiological studies, it was considered of interest to explore the adequacy of the control points classification to exposure percentiles commonly applied in this type of study. These ranges were delimited by magnetic field values: <0.1 μT; 0.1- <0.2 μT; 0.2- <0.4 μT; ≥ 0.4 μT (Ahlbom et al., 2000; Greenland et al., 2000). Other subdivisions were added in the lower levels of classification, corresponding to <0.02 μT and 0.02–0.1 μT included in the standard of the Institute of "Baubiologie & Nachhaltigkeit" (IBN, 2015). Once the surfaces were reclassified according to this categorization, it was examined through a spatial belonging operation to assess how well these areas included the corresponding observations. The result in the urban residential area was that for the magnetic field surfaces generated from DTM05, 86% of the estimates were correctly classified. For the DTM25-based surface, the correct fit of the classification decreased to 71%. For the points distributed in transects lateral to the line, the correspondence was 100% in all cases, although it must be considered that in this validation area all the control points were very close to the power line, so the possibility of belonging to other exposure categories was very slim. Regardless of the assumption, all measured values were well below the maximum exposure limits recommended by the European Union (European Commission, 1999).

4. Discussion

This work has shown that it is possible to generate with a reliable relative accuracy a magnetic field surface generated by HVOPLs in a complex urban area and that it can be addressed exclusively through a Geographic Information System. The proposed procedure integrates a simplified calculation method without the need to resort to specific software to calculate magnetic field values, although it requires that the geometry of the line and the terrain be considered and reproduced from high precision data.

In this way, it is possible to provide not only values in representative specific locations of cases and control for epidemiological studies, but also to provide a representative map of this continuous variable in a sufficiently wide surrounding of the HVOPL to where the magnetic field falls to negligible values. This represents a contribution to the development of the exposure mapping to ELF-MF, neglected in this research field (Kokate et al., 2016).

The magnetic field surfaces have been calculated at 1 m above the ground of the studied area, although it is possible to apply the same procedure described in this work to obtain them at the same ground

Fig. 8. Scatter diagrams of the modelled magnetic field values versus those measured at the control locations in the urban free zone (left) and in the urban residential zone (right).

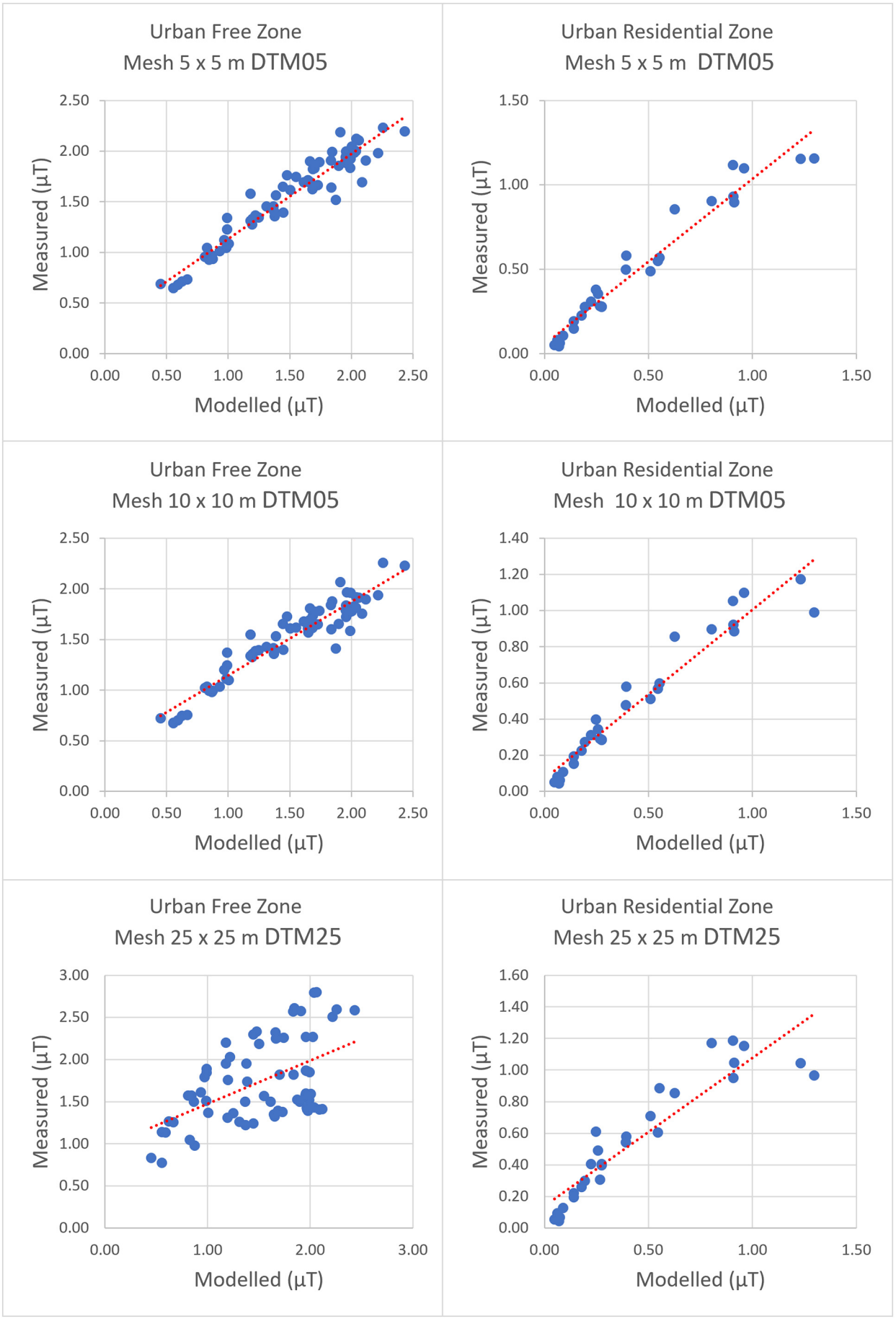
Urban Free Zone
Mesh 5 x 5 m DTM05
Measured (µT)
Modelled (µT)
0.00
0.50
1.00
1.50
2.00
2.50
Urban Residential Zone
Mesh 5 x 5 m DTM05
Measured (µT)
Modelled (µT)
0.00
0.50
1.00
1.50
Urban Free Zone
Mesh 10 x 10 m DTM05
Measured (µT)
Modelled (µT)
0.00
0.50
1.00
1.50
2.00
2.50
Urban Residential Zone
Mesh 10 x 10 m DTM05
Measured (µT)
Modelled (µT)
0.00
0.20
0.40
0.60
0.80
1.00
1.20
1.40
Urban Free Zone
Mesh 25 x 25 m DTM25
Measured (µT)
Modelled (µT)
0.00
0.50
1.00
1.50
2.00
2.50
3.00
Urban Residential Zone
Mesh 25 x 25 m DTM25
Measured (µT)
Modelled (µT)
0.00
0.20
0.40
0.60
0.80
1.00
1.20
1.40
1.60

elevation collected in the reference DTM, and in general, to whatever altitude can be of interest.

It is important to bear in mind that the surfaces generated were only representative when the heights of the bases of the power lines and the ground were derived from a 5 × 5 m resolution DTM. In a validation process of a model for long-term exposure to magnetic fields generated by overhead power lines carried out in Switzerland (Bürgi et al., 2017), the need to use a high precision digital terrain model was concluded. The results were also significantly more accurate when using a 5 × 5m DTM rather than a 25 × 25 m DTM. This later model was used in this case only to obtain the elevation of the HVOPLs supports.

When a higher resolution DTM was used for modelling, the mesh density used to interpolate the magnetic field surface had no significant repercussion in its quality. This observation is important when the methodology proposed in this study is applied to large areas, because the use of a lesser amount of interpolation points can reduce the processing times considerably. Specifically, the IDW interpolation method applied using the ArcGIS 10.7 software has a limit of approximately 45 million input points; although, it is possible to avoid this limit by interpolating the study area in several parts, ensuring that there is some overlapping at the edges, and then creating a mosaic of the results to generate a single large raster dataset (ESRI, 2016). The selected 5 × 5 m mesh covered 189,165 points and the 10 × 10 m mesh, 47,303 points, both for 1000 m on each side of 2.5 km of power line. Thus, it would be feasible for this model to cover the lengths of power lines from a national study, with 5 datasets being enough to address 10,000 km of power lines with a breadth of 1 km on each side of them. An epidemiological study carried out in the United Kingdom (Swanson, 2008) considered 7000 km of power lines and another carried out in France (Bessou et al., 2013) covered 81,000 km of power lines. In addition, the interpolation times of the DTMs orthometric heights, B values calculations and surfaces generation for meshes were of only a few seconds and the proximity to the catenary analyses with an Intel i5-7200U desktop processor did not exceed five minutes. A 10-m mesh magnetic field surface generation performed for the Flanders region (Belgium) using a QSIG plug-in (Joseph et al., 2018) required approximately 14 h with an Inteli7–4770 processor, although without considering the elevation of the terrain. On the other hand, it would also be possible to apply the present methodology for case studies and disease control associated with exposure to ELF-MF in large territories, generating meshes only around the locations of interest where it is desired to estimate the magnetic field, thus considerably reducing the number of points to be processed.

Another relevant factor in the behaviour of the surfaces generated in this work was the type of the urban area modelled. The mean relative error in absolute terms went from 10% in a free urban area to 20% in a consolidated urban area. Although the process for taking the reference B values was carried out in different time periods of the same day for each zone (morning and afternoon), the charge values of the power line did not show in any case significant fluctuations that could affect this difference in results. On the other hand, obtaining DTMs from Light Detection and Ranging (LIDAR) data is especially complex in urban environments (Chen et al., 2017) due to the truly diverse characteristics of its surface such as heterogeneous building distributions, trees, short walls or cables (Meng et al., 2010), which can have repercussions in its quality and, therefore, in the products derived from it.

There are also other important factors to consider. One was that in the urban area there could be an uncontrollable presence of conductive and/or magnetizable elements near the control points, much less important than when working in the open field. The study does not capture the effect of the earth, which becomes important at longer distances. The values studied in the profiles perpendicular to the electrical line were relatively close to it so this effect was negligible, while in the second sample, there were locations where the image of the conductor on the ground could have a certain effect on the error of the order of 3% in exponential growth from 150 to 400 m depending on the ground resistivity (Cruz-Romero, 2000).

The strength of the method for calculating the magnetic fields generated by overhead power lines adopted in this work is that these values can be easily determined by analytical means, but knowledge of the phase configurations is essential, since the B values between one type of configuration and another may differ by a factor of 5 (Bürgi et al., 2017). In case of not knowing the disposition of the phases and/or in complex electrical line layouts (intersecting lines, relatively close parallel lines) it would be necessary to resort to 3D calculation methods (Modrić et al., 2015). However, the integration of a three-dimensional urban model in a geographic information system allows knowing, through spatial analysis operations, the proximity of the study locations to areas with lines that meet certain characteristics and, thus, consider the most appropriate calculation method for each situation. Likewise, in case of not having data for the line charge and the phases configuration, this model allows obtaining precise Euclidean distances between any point on the ground and the power line. These distances can be a predictor of residential exposure to the ELF-MF even more representative than mere horizontal distance.

The maps generated in this work represent the average value of magnetic field for the studied residential area in a time space of a specific day. In this sense, for its possible application in epidemiological studies, it is still necessary to investigate the precision of the obtained results when historical series of line charge values are considered. Currently, 85% of the points observed were correctly classified according to an exhaustive number of magnetic field exposure levels.

Although the temporal approach does not make it completely comparable with this work, other authors (Vergara et al., 2015) who assessed in their model the possibility of the erroneous classification of the exposure having estimated it with 3D calculation methods, obtained a 12% overestimation considering the single exposure percentile ≥0.4 μ. That same study also indicated a Pearson correlation coefficient of 0.78 when comparing the calculated fields with those observed at home visits. It improved to 0.90 when questionable observations were excluded. In this study the agreement was somewhat higher and although the sample was significantly smaller, 28 measurements versus 118, it was consistent with the scale of the study area.

Another model also developed to obtain long-term exposure estimates showed deviations from the magnetic field measurements of ± 1–2% ± 8% (Bürgi et al., 2017), of ±7% ± 1ηT (Swanson, 2008), both for a profile transverse to the line in a non-built area.

In any case, this work provides another representation of how the coefficient of determination (R^2), although statistically significant, does not necessarily evaluate the simulation capacity of a model for a geophysical variable such as magnetic field, and that it is necessary to provide other indicators that allow a more reliable interpretation of the goodness of their predictions, such as the mean relative error and the mean absolute percentage error.

In the literature, not only there is no consensus when it comes to characterizing residential exposure to magnetic fields generated by HVOPLs, but there is also no standardized procedure to assess the representativeness of the proposed magnetic field models and to allow them to be compared more closely. The presence of standards in this sense that include guidelines on the validation procedure of these models (samples according to different distances to the line, reliability indicators to be provided, types of areas where to validate - urbanized or not -, etc.) would allow this task and this would contribute to the development of more precise models of exposure to ELF-MF.

The limitations of our study are mainly subject to the availability, quality and processing of the data. If the geometric and mechanical parameters of the catenary are not available (free height of supports, phase separation, mechanical tension of the cables), it is not possible to carry out its three-dimensional modelling if this information is not obtained from in situ measurements which might not be feasible in large-scale works. If it is based on assumed values, it could affect the

validity of the results. It is necessary to conduct and test this model considering common geometric values from de power line. On the other hand, even having access to real data, modelling an electric power transmission and distribution line on a national scale must entail a significant effort. Also, although for this validation a complex urban area has been chosen as a representation of the most unfavourable scenario, repeat this work in areas with different environments, including densely vegetated countryside and homogeneous layouts of multistorey buildings, is necessary to assess how generalizable this model is. Further testing in clear and flat terrain is also needed to assess in which environments our model is more accurate than others that do not consider the terrain but apply methods for calculating MF intensity values more sophisticated. Also, in the same way when historical series of line load data are considered to obtain long-term exposure averages. Other limitation regarding the method for calculate MF should need to be recognised. The series expansion of the Biot-Savart law applied to indefinite rectilinear conductors, even taking into account variable height according to the catenary described by the cables, is only valid at distances larger in comparison to the spacings between phases. Therefore, our model is not suitable to study the MF exposure in ecosystems very close to the conductors, such as bird nesting in electric power supports.

When it is possible to overcome these limitations, the results obtained have shown that through the methodology applied in this work it is possible to obtain precise MF maps, which could be used in environmental policy to improve public information (European Parliament, 2009), urban planning regarding HVOPLs (PACE, 2011) and the comparison of terrestrial ecosystems before and after a new installation and/or located at different intensities of ELF-MF (SCENIHR, 2009).

5. Conclusions

Modelling the characterization of residential exposure to ELF-MF generated by HVOPLs in large territories is an enormously complex task that requires a significant investment of resources, especially when studying the surroundings closest to these lines. Regardless of whether it is done by estimating magnetic field values or by proxy based on proximity, the high sensitivity of these fields to the distance from their emitting source means that these distances must be reproduced as accurately as possible. In urban areas of complex relief, even if the sag of the overhead power line is reproduced, omitting the consideration of the geographical relief can be a cause of ELF-MF erroneous estimates. On-site inspections or the application of terrain slope correction factors adopted by some studies can be reduced or eliminated by digitally incorporating into the geographic modelling the terrain relief for the entire area of interest.

In this work a model has been provided through a Geographic Information System that solves this challenge and allows to obtain MF values in specific geographic locations and maps at various scales. Also, it allows addressing and investigating the characterization of residential exposure to ELF-MF as the Euclidean distance between receiver-emitter when line charge data is not available, thus refining the concept of proximity.

The need to continue investigating the possible adverse health effects of these fields and their possible combined effect with other environmental pollution factors, as well as the urban planning needs due to the important expansion of many cities towards the surroundings of high voltage electricity meshes, make this work a tool of special interest.

CRediT authorship contribution statement

Laia Miravet-Garret: Conceptualization, Methodology, Validation. **Óscar David de Cózar-Macías:** Validation, Writing – original draft. **Elidia Beatriz Blázquez-Parra:** Supervision. **Manuel Damián Marín-Granados:** Software, Formal analysis. **Juan Bernabé García-González:** Validation, Resources.

Declaration of competing interest

The authors declare that they have no known competing financial interests or personal relationships that could have appeared to influence the work reported in this paper.

Acknowledgments

The authors wish to thank the company e-Distribución Redes Digitales SLU for providing all the technical data of the electrical line studied. Thanks to their support, it has been possible to develop this research. Likewise, they also want to express gratitude to the University of Malaga and CBUA (Consorcio de Bibliotecas Universitarias de Andalucía), for providing all the necessary equipment and publishing support for this work (funding for open access charge: Universidad de Málaga / CBUA).

References

Ahlbom, A., Day, N., Feychting, M., Roman, E., Skinner, J., Dockerty, J., Linet, M., Mcbride, M., Michaelis, J., Olsen, J.H., Tynes, T., Verkasalo, P.K., 2000. A pooled analysis of magnetic fields and childhood leukaemia. Br. J. Cancer 83, 692–698. https://doi.org/10.1054/bjoc.2000.1376.

Ahlbom, A., Cardis, E., Green, A., Linet, M., Savitz, D., Swerdlow, A., 2001. Review of the epidemiologic literature on EMF and health. Environ. Health Perspect. https://doi.org/10.1289/ehp.109-1240626.

Amoon, A.T., Swanson, J., Vergara, X., Kheifets, L., 2020. Relationship between distance to overhead power lines and calculated fields in two studies. J. Radiol. Prot. 40, 431–443. https://doi.org/10.1088/1361-6498/ab7730.

Azpurua, M., dos Ramos, K., 2010. A comparison of spatial interpolation methods for estimation of average electromagnetic field magnitude. Prog. Electromagn. Res. https://doi.org/10.2528/PIERM10083103.

Bessou, J., Deschamps, F., Figueroa, L., Cougnaud, D., 2013. Methods used to estimate residential exposure to 50 Hz magnetic fields from overhead power lines in an epidemiological study in France. J. Radiol. Prot. 33, 349–365. https://doi.org/10.1088/0952-4746/33/2/349.

Bürgi, A., Sagar, S., Struchen, B., Joss, S., Röösli, M., 2017. Exposure modelling of extremely low-frequency magnetic fields from overhead power lines and its validation by measurements. Int. J. Environ. Res. Public Health 14. https://doi.org/10.3390/ijerph14090949.

Chen, Z., Gao, B., Devereux, B., 2017. State-of-the-art: DTM generation using airborne LIDAR data. Sensors (Switzerland) https://doi.org/10.3390/s17010150.

Comelli, M., Benes, M., Bampo, A., Villalta, R., 2007. A technical note about Phidel: a new software for evaluating magnetic induction field generated by power lines. Radiat. Prot. Dosim. 123, 182–189. https://doi.org/10.1093/rpd/ncl111.

Crespi, C.M., Vergara, X.P., Hooper, C., Oksuzyan, S., Wu, S., Cockburn, M., Kheifets, L., 2016. Childhood Leukaemia and Distance from Power Lines in California: A Population-Based Case-Control Study. vol. 115. https://doi.org/10.1038/bjc.2016.142.

Cruz-Romero, P., 2000. Análisis, cálculo y técnicas de mitigación de campos magnéticos creados por líneas eléctricas de alta tensión.

Draper, G., Vincent, T., Kroll, M.E., Swanson, J., 2005. Childhood cancer in relation to distance from high voltage power lines in England and Wales: a case-control study. BMJ 330, 1290. https://doi.org/10.1136/bmj.330.7503.1290.

ESRI, 2016. IDW—raster interpolation toolset [WWW document]. URL. https://desktop.arcgis.com/en/arcmap/10.3/tools/3d-analyst-toolbox/idw.htm.

European Commission, 1999. CELEX1, 1999/519/CE: Recomendación del Consejo, de 12 de julio de 1999, relativa a la exposición del público en general a campos electromagnéticos (0 Hz a 300 GHz).

European Commission, 2010. Special Eurobarometer 347 / Wave 73.3 – TNS Opinion & Social. Bruxelles.

European Parliament, 2009. P6_TA(2009)0216 Health Concerns Associated with Electromagnetic Fields.

Feychting, M., 2014. Selection and detection Bias. In: Roosli, M. (Ed.), Epidemiology of Electromagnetic Fields, pp. 57–65.

Feychting, M., Alhbom, M., 1993. Magnetic fields and cancer in children residing near Swedish high-voltage power lines. Am. J. Epidemiol. 138, 467–481. https://doi.org/10.1093/oxfordjournals.aje.a116881.

Furby, L., Slovic, P., Fischhoff, B., Gregory, R., 1988. Public perceptions of electric power transmission lines. J. Environ. Psychol. 8, 19–43. https://doi.org/10.1016/S0272-4944(88)80021-5.

Graham, A.J., Atkinson, P.M., Danson, F.M., 2004. Spatial analysis for epidemiology. Acta Trop. https://doi.org/10.1016/j.actatropica.2004.05.001.

Greenland, S., Sheppard, A.R., Kaune, W.T., Poole, C., Kelsh, M.A., 2000. A pooled analysis of magnetic fields, wire codes, and childhood leukemia. Epidemiology 11, 624–634. https://doi.org/10.1097/00001648-200011000-00003.

Hoffmann, W., Terschüeren, C., Heimpel, H., Feller, A., Butte, W., Hostrup, O., Richardson, D., Greiser, E., 2008. Population-based research on occupational and environmental factors for leukemia and non Hodgkin's lymphoma: the northern Germany leukemia and lymphoma study (NLL). Am. J. Ind. Med. 51, 246–257. https://doi.org/10.1002/ajim.20551.

IARC, 2002. Non-ionizing Radiation, Part 1: Static and Extremely Low-Frequency (ELF) Electric and Magnetic Fields. IARC Monographs on the Evaluation of Carcinogenic Risks to Humans. World Health Organization, International Agency for Research on Cancer https://doi.org/10.1097/00004032-200212000-00021.

IARC, 2013. Non-ionizing Radiation, Part 2: Radiofrequency Electromagnetic Fields. IARC Monographs on the Evaluation of Carcinogenic Risks to Humans. World Health Organization, International Agency for Research on Cancer.

IBN, 2015. Building Biology Evaluation Guidelines for Sleeping Areas (SBM-2015).

IEEE Std 644-1994, 1994. IEEE Standard Procedures for Measurement of Power Frequency Electric and Magnetic Fields from AC Power Lines Transmission and Distribution.

Jerrett, M., Gale, S., Kontgis, C., 2010. Spatial modeling in environmental and public health research. Int. J. Environ. Res. Public Health 7, 1302–1329. https://doi.org/10.3390/ijerph7041302.

Joseph, W., Vanhecke, K., Geuzaine, C., Verloock, L., van den Bossche, M., Verlaek, M., Goethals, M., Martens, L., 2018. QGIS Calculation Method for Evaluation of ELF Electromagnetic Field Exposure of General Public Due to Overhead Power Lines.

Kaune, W.T., Zaffanella, L.E., 1992. Analysis of magnetic fields produced far from electric power lines. IEEE Transactions on Power Delivery. 7, pp. 2082–2091. https://doi.org/10.1109/61.157011.

Kheifets, L., Kavet, R., Sussman, S.S., 1997. Wire Codes, Magnetic Fields, and Childhood Cancer, Bioelectromagnetics. Wiley-Liss, Inc.

Kheifets, L., Crespi, C.M., Hooper, C., Oksuzyan, S., Cockburn, M., Ly, T., Mezei, G., 2015. Epidemiologic study of residential proximity to transmission lines and childhood cancer in California: description of design, epidemiologic methods and study population. J. Expo. Anal. Environ. Epidemiol. 25, 45–52. https://doi.org/10.1038/jes.2013.48.

Kokate, P.A., Mishra, A.K., Lokhande, S.K., Bodhe, G.L., 2016. Extremely low frequency electromagnetic field (ELF-EMF) and childhood leukemia (CL) near transmission lines: a review. Advanced Electromagnetics https://doi.org/10.7716/aem.v5i1.348.

Lienert, P., Sütterlin, B., Siegrist, M., 2017. Public Acceptance of High-Voltage Power Lines: The Influence of Information Provision on Undergrounding. https://doi.org/10.1016/j.enpol.2017.10.025.

Mamishev, A.v., Nevels, R.D., Russell, B.D., 1996. Effects of conductor sag on spatial distribution of power line magnetic field. IEEE Transactions on Power Delivery. 11, pp. 1571–1576. https://doi.org/10.1109/61.517518.

Maslanyj, M., Simpson, J., Roman, E., Schüz, J., 2009. Power frequency magnetic fields and risk of childhood leukaemia: misclassification of exposure from the use of the "distance from power line" exposure surrogate. Bioelectromagnetics 30, 183–188. https://doi.org/10.1002/bem.20465.

Meng, X., Currit, N., Zhao, K., 2010. Remote sensing ground filtering algorithms for airborne LiDAR data: a review of critical issues. Remote Sens. 2, 833–860. https://doi.org/10.3390/rs2030833.

Modrić, T., Vujević, S., Lovriè, D., 2015. 3D computation of the power lines magnetic field. Prog. Electromagn. Res. 41, 1–9. https://doi.org/10.2528/PIERM14122301.

Najjar, M.B., Jadayel, O., Baarini, A., 2009. Power Magnetic Fields Exposure Evaluation at North Lebanon: GIS Application.

PACE, 2011. Resolution 1815: The Potential Dangers of Electromagnetic Fields and their Effect on the Environment.

PCE Instruments, 2014. Tester de radiación PCE-G28 [WWW Document]. URL. https://www.pce-iberica.es/medidor-detalles-tecnicos/instrumento-de-radiacion/tester-de-radiacion-828.htm (accessed 6.9.21).

Pedersen, C., BräUner, E. v, Rod, N.H., Albieri, V., Andersen, C.E., Ulbak, K., Hertel, O., Johansen, C., Schü, Z.J., Raaschou-Nielsen, O., 2014a. Distance to High-Voltage Power Lines and Risk of Childhood Leukemia-an Analysis of Confounding by and Interaction with Other Potential Risk Factors. https://doi.org/10.1371/journal.pone.0107096.

Pedersen, C., Raaschou-Nielsen, O., Rod, N.H., Frei, P., Poulsen, A.H., Johansen, C., Schüz, J., 2014b. Distance from residence to power line and risk of childhood leukemia: a population-based case-control study in Denmark. Cancer Causes Control 25, 171–177. https://doi.org/10.1007/s10552-013-0319-5.

Pontius, R.G., Thontteh, O., Chen, H., 2008. Components of information for multiple resolution comparison between maps that share a real variable. Environ. Ecol. Stat. 15, 111–142. https://doi.org/10.1007/s10651-007-0043-y.

Porsius, J.T., Claassen, L., Smid, T., Woudenberg, F., Timmermans, D.R.M., 2014. Health responses to a new high-voltage power line route: design of a quasi-experimental prospective field study in the Netherlands. BMC Public Health 14, 1–12. https://doi.org/10.1186/1471-2458-14-237.

Rankin, R.F., Bracken, T.D., Senior, R.S., Kavet, R., Montgomery, J.H., 2002. Results of a multisite study of U.S. residential magnetic fields. J. Expo. Anal. Environ. Epidemiol. 12, 9–20. https://doi.org/10.1038/sj/jea/7500196.

Repacholi, M., 2012. Concern that "EMF" magnetic fields from power lines cause cancer. Sci. Total Environ. 426, 454–458. https://doi.org/10.1016/j.scitotenv.2012.03.030.

Reynolds, P., Elkin, E., Scalf, R., von Behren, J., Neutra, R.R., 2001. A case-control pilot study of traffic exposures and early childhood leukemia using a geographic information system. Bioelectromagnetics (Suppl. 5) https://doi.org/10.1002/1521-186X(2001)22:5+<::AID-BEM1024>3.3.CO;2–0.

SCENHIR, 2015. Opinion on Potential Health Effects of Exposure to Electromagnetic Fields (EMF). https://doi.org/10.2772/75635.

SCENIHR, 2009. Research Needs and Methodology to Address the Remaining Knowledge Gaps on the Potential Health Effects of EMF.

Schüz, J., Dasenbrock, C., Ravazzani, P., Röösli, M., Schär, P., Bounds, P.L., Erdmann, F., Borkhardt, A., Cobaleda, C., Fedrowitz, M., Hamnerius, Y., Sanchez-Garcia, I., Seger, R., Schmiegelow, K., Ziegelberger, G., Capstick, M., Manser, M., Müller, M., Schmid, C.D., Schürmann, D., Struchen, B., Kuster, N., 2016. Extremely low-frequency magnetic fields and risk of childhood leukemia: a risk assessment by the ARIMMORA consortium. Bioelectromagnetics https://doi.org/10.1002/bem.21963.

Sermage-Faure, C., Demoury, C., Rudant, J., Goujon-Bellec, S., Guyot-Goubin, A., Deschamps, F., Hemon, D., Clavel, J., 2013. Childhood leukaemia close to high-voltage power lines - the Geocap study, 2002-2007. Br. J. Cancer 108, 1899–1906. https://doi.org/10.1038/bjc.2013.128.

Swanson, J., 2008. Methods used to calculate exposures in two epidemiological studies of power lines in the UK. J. Radiol. Prot. 28, 45–59. https://doi.org/10.1088/0952-4746/28/1/002.

Teepen, J.C., van Dijck, J.A.A.M., 2012. Impact of high electromagnetic field levels on childhood leukemia incidence. Int. J. Cancer https://doi.org/10.1002/ijc.27542.

Turgeon, A., Maruvada, P.S., Goulet, D.L., 1998. Application of GIS for the evaluation of human exposure to magnetic field in the vicinity of power lines. Canadian Conference on Electrical and Computer Engineering. IEEE, pp. 189–192 https://doi.org/10.1109/ccece.1998.682714.

Tynes, T., Haldorsen, T., 1997. Electromagnetic fields and cancer in children residing near Norwegian high-voltage power lines. Am. J. Epidemiol. 145 (3), 219–226. https://doi.org/10.1093/oxfordjournals.aje.a009094.

UNE 215001:2004, 2004. Procedimientos normalizados para la medida de los campos eléctricos y magnéticos de frecuencia industrial producidos por las líneas eléctricas de alta tensión.

Vergara, X.P., Kavet, R., Crespi, C.M., Hooper, C., Michael Silva, J., Kheifets, L., 2015. Estimating magnetic fields of homes near transmission lines in the California Power Line Study. Environ. Res. 140, 514–523. https://doi.org/10.1016/j.envres.2015.04.020.

Wertheimer, N., Leeper, E., 1979. Electrical wiring configurations and childhood cancer. Am. J. Epidemiol. 109, 273–284. https://doi.org/10.1093/oxfordjournals.aje.a112681.

Wertheimer, Nancy, Leeper, Ed, 1982. Adult cancer related to electrical wires near the home. Int. J. Epidemiol. 11, 345–355. https://doi.org/10.1093/ije/11.4.345.

WHO, 2007. Environmental Health Criteria 238. Extremely Low Frequency Fields (Geneva).

Willmott, C.J., 1982. Some comments on the evaluation of model performance. Bull. Am. Meteorol. Soc. 63, 1309–1313. https://doi.org/10.1175/1520-0477(1982)063<1309:SCOTEO>2.0.CO;2.